Light-inducible T cell engagers trigger, tune and shape the activation of primary T cells

Morgane Jaeger[1], Amandine Anastasio[1], Sophie Brustlein[2], Renaud Vincentelli[3], Fabien Durbesson[3], Rémy Char[1], Maud Boussand[1], Mathias Lechelon[1], Rafael J. Argüello[1], Didier Marguet[1], Hai-Tao He[1] and Rémi Lasserre[1*]

[1]Aix Marseille Université, Centre National de la Recherche Scientifique (CNRS), Institut National de la Santé et de la Recherche Médicale (Inserm), Centre d'Immunologie de Marseille Luminy (CIML), CENTURI, Marseille, France.

[2]Aix Marseille Université, Institut National de la Santé et de la Recherche Médicale (Inserm), Institut de neurobiologie de la Méditerranée (Inmed), CENTURI, Marseille, France.

[3]Aix Marseille Université, Centre National de la Recherche Scientifique (CNRS), Architecture et Fonction des Macromolécules Biologiques (AFMB), Marseille, France.

[*]Corresponding author: lasserre@ciml.univ-mrs.fr

Cells perceive overtime complex sequences of receptor stimulation that they integrate to mount an appropriate response. Yet, the influence of signal dynamics on cell responses has been poorly characterized due to technical limitations. Here, we present a generalizable approach to control receptor stimulation on unmodified primary cells. Indeed, for applications on primary murine T cells, we have engineered the LiTe system, a new recombinant optogenetics-based Light-inducible T cell engager which allows tunable and reversible spatiotemporal control of the T Cell Receptor (TCR) stimulation. We also provided *in vitro* evidence that this system enables efficient T cell activation with light, leading to cytokine secretion or tumor cell killing. Using specific time-gated stimulations, we have been able to orient the outcome of the activation of T cells. Overall, the LiTe system constitutes a versatile ON/OFF molecular switch allowing to decipher the cellular response to stimulation dynamics. Its original control over T cell activation opens new avenues for future precision cancer immunotherapy.

In addition to the nature and intensity of a stimulus, its dynamic features (frequency, duration) also constitute a layer of information that is decoded by cells and translated into specific outcomes [1]. *In vivo*, T cell activation is usually initiated through transient and sequential interactions with different APCs presenting cognate pMHC ligands [2-4]. During these interactions, TCR signaling is triggered [5] and T cells appear able to integrate, or sum, the signals perceived during a series of TCR stimulations [6-9]. This TCR stimulation dynamics is thought to influence the outcome of the T cell activation [2, 10], yet a causal relation has not been formally demonstrated. Indeed, approaches for accurate and reversible spatiotemporal manipulation of primary cell stimulations are still missing, hampering the characterization of the cellular mechanisms responsible for the integration of activation signals and of the influence of signal dynamics on activation outcome.

Optogenetics is a technology based on the use of light-responsive protein domains from plants, algae or prokaryotes, to confer a light-responsive capacity to targeted biological processes. It offers spatiotemporal control with light of cellular activities, opening new opportunities in basic and biomedical research. However, these elegant approaches are often limited by the need to transduce genes encoding engineered light-responding proteins, making it difficult to manipulate unmodified primary cells [8, 11-16]. Here, we describe a novel strategy to control receptor stimulation on unmodified primary cells with light.

We engineered the LiTe system, a recombinant and reversible light-inducible stimulatory system to control the activation of unmodified primary T cells. Its rationale relies on the fact that a non-agonist monovalent Fab can become a potent agonist upon oligomerization [17]. The LiTe system has two components: (i) the N-terminal phytochrome B_{1-651} region from *A. thaliana* linked to the phycocyanobilin (PhyB) and (ii), the LiTe protein that combines the phytochrome interacting factor 6 (PIF6) with the Fab fragment from the H57 mAb, an agonist targeting the mouse TCR β-chain (Fig. 1a and Supplementary Fig. 1). Under red light illumination (e.g. 656 nm), PhyB will capture the PIF6 domain of the LiTe protein, but far-red illumination will abrogate this interaction. Once the LiTe proteins bind TCRs, their light-controlled capture by PhyB-coated supports will induce reversible TCR triggering (Fig. 1b). We validated the ability of the LiTe protein to bind specifically to the TCR (Supplementary Fig. 2a,b). We also verified that its interaction with PhyB occurred only under red light exposure (Supplementary Fig. 2c,d).

We evaluated the LiTe system on living primary T cells by recording its ability to trigger intracellular calcium influx as an early, sensitive and dynamic readout of TCR engagement [9, 18, 19]. Primary $CD8^+$ T cells were loaded with PBX calcium-sensitive dye and the LiTe before incubated with PhyB-coated beads and imaged by videomicroscopy at 37°C. Switching light from 740 nm to 656 nm triggered an increase in intracellular calcium within tens of seconds solely for T cells in contact with PhyB-coated beads (Fig. 1c and Supplementary Fig. 3). The calcium concentration gradually returned to the basal level within two minutes after switching back light to 740 nm. This observed dynamics is consistent with previous observations for TCR-induced calcium flux during antigen recognition [9, 18, 19]. Moreover, by applying iterative cycles of 656/740 nm light exposures, the LiTe system made it possible to deliver pulsed stimuli to T cells as evidenced by intracellular calcium fluxes that perfectly matched the dynamics of light cycles (Fig. 1d). Also, under 656 nm light, the shape of T cells in contact with PhyB-coated beads was reminiscent of that reported at the immunological synapse; this suggests that numerous TCRs were engaged (Fig. 1e). Altogether, these observations demonstrate that the LiTe system constitutes an ON/OFF molecular switch enabling precise spatiotemporal control of T cell activation by delivering strong, reversible and iterative TCR stimulation. More importantly, this optogenetic tool has the unique ability to operate on primary T cells without requiring their genetic manipulation.

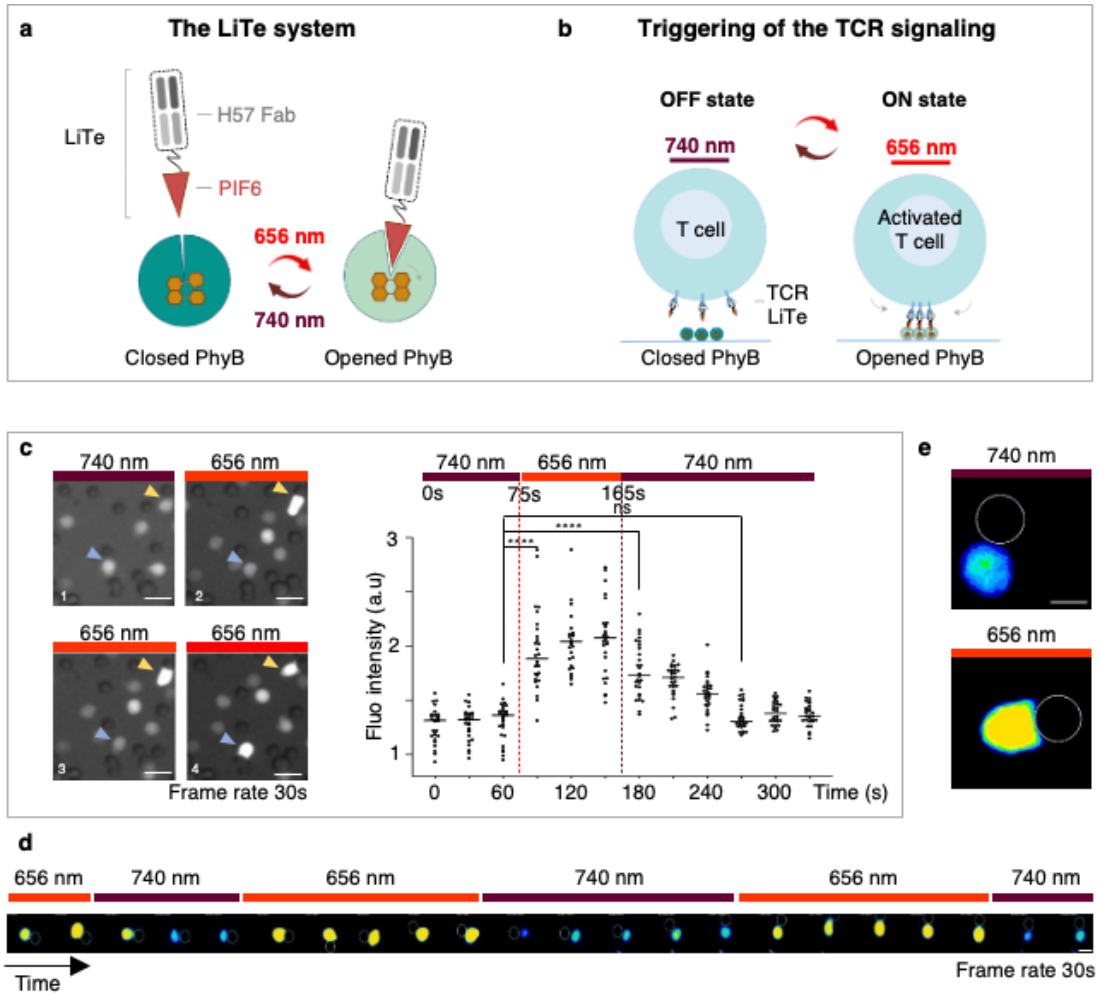

Figure 1 | Design of the LiTe system for reversible triggering of TCR signaling in response to light. a, The LiTe system is in two parts: LiTe protein, a recombinant protein linking the PIF6 domain to the anti-mouse TCR H57-597 Fab and $PhyB_{1-651}$. Exposure of the LiTe system to red light opens the PhyB binding site for PIF6 whereas far-red light reverses its conformational change. **b**, Exposure of mouse T cells in presence of the LiTe system to 656 nm light induces the binding of TCR-bound LiTe proteins to PhyB-coated surface, leading to TCR aggregation/immobilization and triggering. This process is reversed by 730-760 nm light. **c**, Primary T lymphocytes were loaded with PBX, a calcium sensitive dye, then incubated with the LiTe protein before been mixed with PhyB-coated beads and imaged by fluorescence microscopy at 37°C. Left panel**,** time-lapse images of the cells exposed to 740 nm light, then to 656 nm light in presence of LiTe system. Arrows specified cells contacting PhyB-coated beads over time. Right panel, quantification of relative fluorescence intensity of cells contacting PhyB-coated beads and exposed to the specified light sources (n = 30 cells, representative of >3 experiments; **** $P < 0.0001$, Wilcoxon- Mann-Whitney test; scale bar: 10 µm). **d**, Time-lapse images of a T cell under iterative stimulation/resting cycles (scale bar: 5 µm, frame rate: 30 s). **e**, Morphological changes triggered by the TCR photostimulation for a cell contacted by PhyB-coated bead under 740 nm (top) or 656 nm (bottom) lights; scale bar: 5 µm.

Efficient T cell stimulation drives the surface expression of activation surface markers and sets effector functions such as cytokine secretion or cytotoxicity. Primary $CD8^+$ T cells were incubated with the LiTe system, in the presence of soluble anti-CD28 mAb that increased the fraction of responding cells (Supplementary Fig. 4). Cells were placed on an illumination device (optoPlate-96, [20]) and illuminated for 18 hours with light at 630 nm (ON), or 780 nm (OFF). Next, T cell activation was assessed by flow cytometric analysis of the surface expression of activation markers (Fig. 2a). Upon 780 nm light, the cells remained in a resting state. In contrast, the 630 nm light triggered potent T cell activation, as evidenced by an increase in CD69 and CD25 expression, and a decrease in CD62-L. Under these conditions, up to 80% T cells were activated as for anti-CD3/anti-CD28 stimulation. As expected, the

630 nm light or LiTe system alone could not induce any T cell activation (Supplementary Fig. 5a). Also, the low light powers used in these experiments (0.14 mW.cm^{-2} at 630 nm and 2.8 mW.cm^{-2} at 780 nm) were not phototoxic (Supplementary Fig. 5b). We then determined whether the LiTe system allows for tuning the activation of T cells under the same experimental conditions but mixing at different ratios of 630 nm/780 nm light powers (Fig. 2b). Flow cytometry analysis of CD69 and CD25 upregulation revealed a dose response on the proportion of activated T cells as a function of the ratio 630 nm/780 nm light powers. Therefore, the LiTe system allowed adjustable control of the extent of T cell activation.

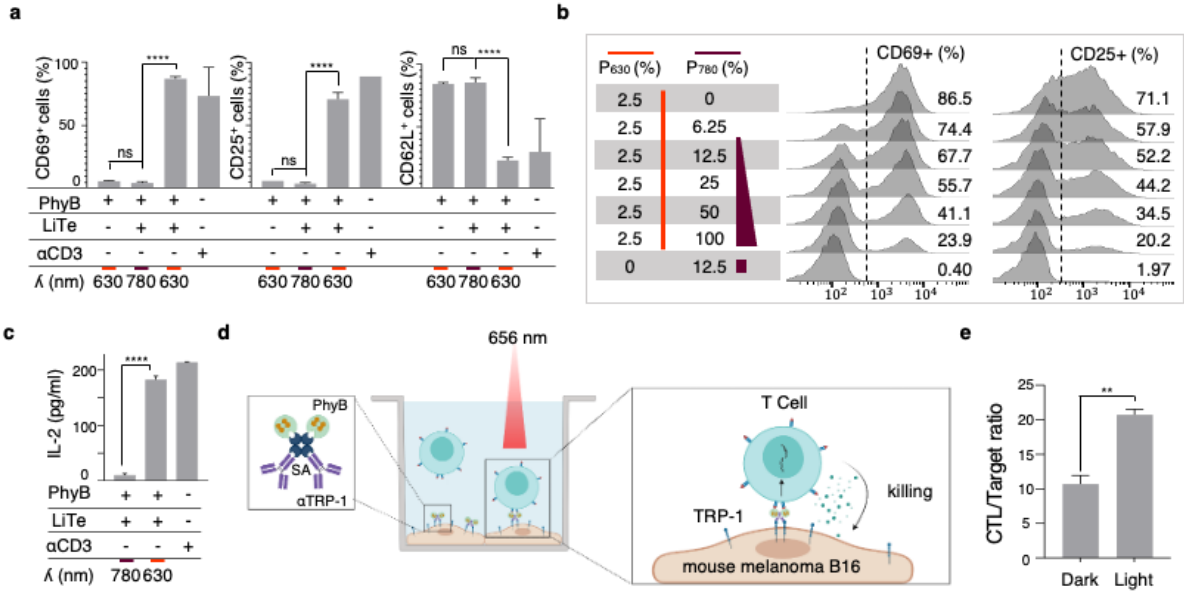

Figure 2 | LiTe-driven TCR photostimulation is tunable and leads to effective T cell activation. a, Primary T cells were incubated with the LiTe system and anti-CD28 antibody, then illuminated 18 h in optoPlate at the specified wavelength. Flow cytometry analysis of CD69, CD25 or CD62L positive cells in response to 630 or 780 nm light (n > 3, mean +/- SEM are shown; *** P < 0.001, **** P < 0.0001, Student t-test). **b**, Same experimental conditions as in **a**, except that cells are exposed to different ratios of 630 nm/780 nm light power (expressed in % of max power intensity) and analyzed for the expression of CD69 or CD25 by flow cytometry. **c**, Same experimental conditions as in **a**, except that IL-2 secretion was analyzed in the cell supernatant by ELISA (n = 3; mean +/- SD are shown; **** P < 0.0001, Student t-test). **d**, LiTe-Me system design. PhyB is combined to Streptavidin (SA) and to the melanoma cell-targeting antibody TA-99 (specific for surface molecule TRP-1). When bound to melanoma cells, the Me-PhyB complex can engage LiTe-bound CTL when exposed to 656 nm light, and trigger tumor cell killing. **e**, CTLs were dropped on a B16F10 melanoma cell monolayer in presence of the LiTe-Me system, illuminated or not with a 656 nm light for 18 h at 37°C. Flow cytometry analysis of the CTL/target cell ratio, identified respectively with anti-CD45 and anti-TRP-1 mAbs (n = 2; mean +/- SD are shown; ** P < 0.001, Student t-test).

To assess the ability of the LiTe system to induce T cell effector functions, we first monitored the cytokine production. Purified primary CD8$^+$ T cells were stimulated as described above with 630 nm light and secreted IL-2 was quantified by ELISA (Fig. 2c). The LiTe system appeared very effective in inducing IL-2 production by the T cells, only when exposed to 630 nm light. Another fundamental effector function of the CD8$^+$ T cell compartment is the killing of target cells, such as cancer cells, through the polarized secretion of cytotoxic granules. Therefore, we evaluated the LiTe system for triggering tumor cell killing by the syngenic CD8$^+$ effector T cell. To target the LiTe to melanoma cells, we generated the LiTe-Me version, in which PhyB is coupled to a mAb specific for TRP-1, a Melanoma-associated antigen (Fig. 2d). To do this, we generated a molecular complex between streptavidin and biotinylated forms of PhyB and anti-TRP-1 mAb (Supplementary Fig. 6). CD8$^+$ effector T cells and the

LiTe-Me system were added on a B16F10 melanoma cell monolayer and illuminated or not with red light for 18 h. Flow cytometry measurement of T cell/B16F10 ratios showed a 2-fold increase only when the cells were in the presence of the LiTe-Me system and illuminated with red light (Fig. 2e).

Altogether, these experiments show that the LiTe system enables specific and adjustable activation of primary T cells, leading to the establishment of their effector functions. LiTe-Me system provides the control of T cell activity in a cell/cell interface, without the use of beads or any artificial surfaces. More importantly, we provide *in vitro* evidence that LiTe-Me acts as a light-inducible Bispecific T cell Engager (BiTE), allowing light-mediated spatiotemporal control of tumor cell killing by CTLs.

Studies suggest that the dynamics of T cells/APCs interactions could influence the outcome of T cell activation[2, 10]. We took advantage of the LiTe system flexibility to explore how the dynamics of the TCR stimulation would influence the outcome of T cell population activation. Our goal was also to determine whether the LiTe system could allow manipulation/orientation of the adaptative immune response.

We first confirmed that PhyB remained functional after hours of exposure to illumination cycles alternating 630 nm and 780 nm lights (Supplementary Fig. 7). Then, purified primary T cells were incubated with the LiTe system and soluble anti-CD28 mAb for 18 h, stimulated with time-gated 630 nm light exposure in continuous or pulsed mode, and their activation analyzed by flow cytometry (Fig. 3a). Upon continuous TCR stimulations, $CD8^+$ and $CD4^+$ T cell subsets activated to a similar extent, although the latter responded slightly better to short stimulations (Fig. 3b).

However, when T cells were exposed to different temporal patterns of pulsed stimulation for 18 h, $CD4^+$ T cells clearly showed a higher response than $CD8^+$ T cells (Fig. 3c). For the short 2 min ON/4 min OFF cycles, the proportion of activated cells was even 2-fold higher in $CD4^+$ than in $CD8^+$ T cell subsets (57% versus 28% of $CD69^+$ cells, respectively). In comparison to continuous stimulations, pulsed stimulations favored the activation of $CD4^+$ T cells over $CD8^+$ T cells, as illustrated by the ratios of activated $CD4^+/CD8^+$ T cells (Fig. 3d). Of note, the duty cycles were held constant (33%, 6 h of cumulated ON state over 18 h of experiment) between different pulse cycles that ranged from 6 to 90 min. The cycle length had only a moderate influence on T cell activation (Fig. 3c).

The differential ability of the T cell subsets to respond to pulsed stimulations rise the possibility of using the LiTe system to qualitatively manipulate the activation of the T cell compartment. We therefore characterized the panel of cytokines produced by primary T cells following the 6 h continuous or the short-pulsed stimulations (iterative 2 min ON/4 min OFF cycles,). Interestingly, pulsed stimulations of T cells induced the production of higher amounts of IL-2 production than continuous stimulations, but lower amounts of IFN-γ, TNF-α, and IL-17 (Fig. 3e,f).

Altogether, these experiments showed that $CD4^+$ T cells have a remarkable ability to integrate a series of short-lived TCR stimulations. They also demonstrated that the dynamics of TCR stimulation directly influences the panel of cytokines secreted by the T cell compartment. Therefore, the LiTe system combined with specific illumination strategies allows manipulation of the activation of the T cell compartment as well as the associated cytokine panel.

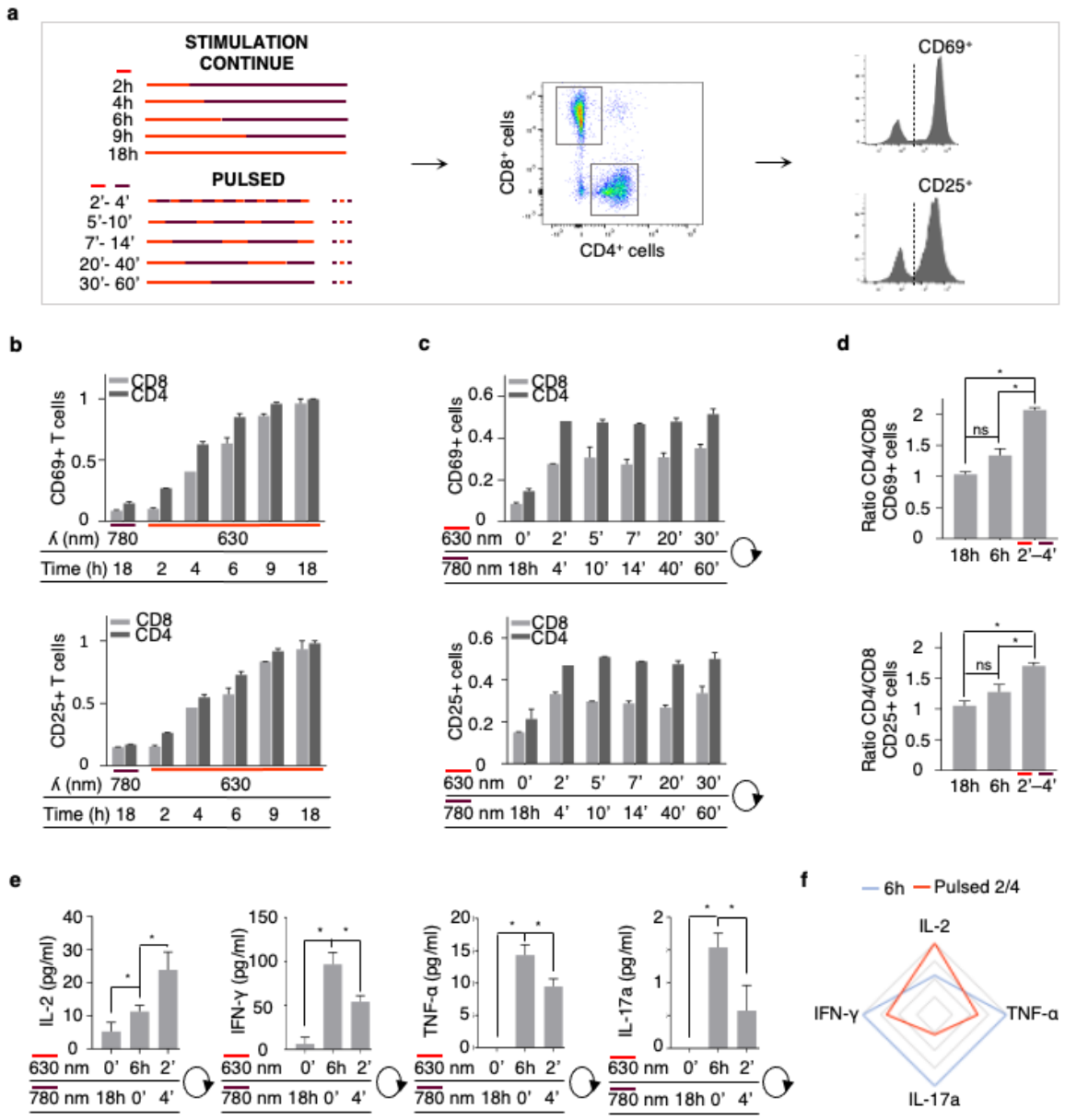

Figure 3 | LiTe system enabled the manipulation of the adaptative immune response. a, Primary T cells were incubated with the LiTe system and anti-CD28 antibody, illuminated for 18 h in optoPlate under continuous or pulsed illumination strategies that all correspond to a 6 h cumulated exposure to 630 nm light. $CD4^+$ and $CD8^+$ T cells subsets were analyzed by flow cytometry for CD69 and CD25 expression. **b**, Flow cytometry analysis of the T cell activation following different times of continuous photostimulation (n > 3; mean +/- SEM are shown; normalized data to 18 h continuous photostimulation value). **c**, same as in **b**, but for pulsed photostimulation of different durations (n > 3; mean +/- SEM; normalized data to 18 h continuous photostimulation value). **d**, Ratio of $CD69^+$ $CD4^+$/ $CD69^+$ $CD8^+$ T cells (upper panel) and $CD25^+$ $CD4^+$/ $CD25^+$ $CD8^+$ T cells (lower panel) under different photostimulation conditions. The 2'-4' pulsed stimulation condition over 18 h correspond to a cumulated 6 h exposure to the 630 nm light (n > 3; mean +/- SD are shown; data normalized to 18 h continuous photostimulation value, * $P < 0.05$, Wilcoxon-Mann-Whitney test). **e**, Measurement of cytokine secretion in the supernatant of T cells stimulated or not 6 h in continuous or pulsed modes. IL-2 has been detected by ELISA, IFN-γ, TNF-α and IL-17 by multiplex assay (n = 2; mean +/- SD; * $P < 0.05$, Wilcoxon-Mann-Whitney test). **f**, Polar representation of the cytokine panels produced by the T lymphocytes stimulated after the continuous (in blue) or the pulsed (in red) stimulations shown in **e** (normalized to the maximum value detected for each cytokine).

Optogenetics is a promising technology for manipulating cellular activity in basic and biomedical research. However, it has been limited, to some degree, by the constraints of genetic modification of cells, making it difficult to study and manipulate primary cells. Our results show that using the fully recombinant LiTe system can overcome this limitation. While we have harnessed it on primary T cells, its modular design allows it to be easily adapted to other biological systems.
By providing the spatiotemporal control of TCR stimulation, the LiTe system enables quantitative, but also qualitative manipulation of the T cell activation. Several studies have suggested that the dynamics of T cell stimulation qualitatively influences their response [2, 10]. Here, we provide direct evidence of a causal relationship linking the dynamics of TCR stimulation and the outcome of T cell activation. Further research is needed to refine our knowledge of this relationship and to determine the extent to which controlling the dynamics of TCR stimulation with the LiTe system would enable to promote an array of T cell activation outcomes (e.g. tolerance, TH-1, TH-2, TH-17 responses…).

In the mouse model, optogenetics is beginning to be applied to onco-immunology research by producing CAR T cells whose activation is inducible by light [16,17,21]. In this context, the LiTe-Me system provided proof of concept of the relevance of optogenetics to also control the bioactivity of BiTEs by light. Such a spatiotemporal targeting of BiTEs activity should limit their adverse effects. Furthermore, the ability to direct the outcome of T-cell activation in response to specific time-gated photostimulations could provide a new level of control of the antitumor immune response. Indeed, differences in the production of IL-2, TNF-α, IL-17 and IFNγ in the tumor bed can have a strong influence in the recruitment and function of bystander T cells, NK cells, macrophages, neutrophils and other stromal cells. Future studies will be necessary to test LiTe-Me *in vivo* and determine the requirements to fully unleash its therapeutic potential. Its regulation with red and far-red lights, which have a good penetration into the tissues, is a great advantage for this purpose [21].

Overall, the LiTe system is an innovative and versatile molecular toolbox that allows precise spatiotemporal control of primary cells. This opens new avenues in biomedical research for the development of future therapeutic approaches.

MATERIALS AND METHODS

Reagents and antibodies

Dulbecco's modified Eagle medium (DMEM), Roswell Park Memorial Institute medium (RPMI), Dulbecco's Modified Eagle Medium/Nutrient Mixture F-12 (DMEM/F-12), sodium pyruvate (NaPy), L-glutamine (L-GLu), penicillin-streptomycin (Pen-Strep), geneticin, HEPES buffer solution, and β2-mercaptoethanol were purchased from Gibco. Phosphate-buffered saline (PBS), streptomycin sulfate salt, biotin, tris (2-carboxyethyl) phosphine (TCEP), Tween 20, valproic acid sodium salt were supplied by Sigma Aldrich. Streptavidin-HRP was purchased from Beckman Coulter. Alexa Fluor 488 and caspase-3/7 activity detection dyes were purchased from Thermo Fischer, Viobility™ 405/452 fixable dye from Miltenyi Biotech.

The monoclonal antibodies anti-CD28 (clone H37.51) and goat anti-mouse IgG antibody HRP were purchased from Thermo Fischer, FITC anti-CD62L (clone MEL-14) from BioLegend, APC anti-CD69 (clone REA937) from Miltenyi, FITC anti-CD25 (clone 7D4) and anti-6xHis (clone F24-796) from BD Biosciences, AF647 anti-histidine (clone AD1.1.10) from Bio-RAD and, APC anti-CD45 (clone 30-F11) from eBioscience™. The TA-99 antibody (α-TRP-1) was a gift from Innate Pharma SA. The anti-TCR β (clone H57-597) and anti-CD3ε (clone 145-2C11) were purified from hybridoma culture supernatants following standard protocols. H57-597 Fab fragment was prepared by papain digestion, purified by ion-exchange, and controlled by SDS-PAGE. Fluorescent labeling of proteins were performed according to manufacturer's instructions.

Cell culture

Melanoma B16F10 cell line was cultured in the RPMI supplemented with 10% fetal bovine serum (FBS) with 7.5% CO_2 at 37°C. The MCD4 cell line was derived from the mouse 3A9 $CD4^+$ T cell hybridoma expressing a high TCR level specific for hen egg lysozyme peptide (HEL) bound to MHC II I-A^k molecules as described [22]. MCD4 were growth in RPMI supplemented with 5% FBS, 1 mM NaPy, 10 mM HEPES with 10% CO_2 at 37°C. The human embryonic kidney 293T cell line (HEK293T) was growth in DMEM supplemented with 10% FBS, 1 mM NaPy, 2 mM L-Glu and geneticin with 7.5% CO_2.

Primary T lymphocytes cells were isolated from lymph nodes of C57BL/6 mice using the Dynabeads™ untouched™ mouse T cell kit (Invitrogen™) by negative selection. $CD8^+$ T cells were isolated from lymph nodes of C57BL/6 $Rag1^{-/+}$ $OT\text{-}1^{-/+}$ mice and purified using the EasySep™ mouse $CD8^+$ T cell isolation kit (STEMCELL Technologies) by negative selection. T cells were cultured in complete DMEM/F-12 medium (DMEM/F-12 supplemented with 10% FBS, 1 mM NaPy, 10 mM HEPES, 50 U/mL Pen-Strep, 0.05 mM β2-mercapto-ethanol) with 10% CO_2 at 37°C.

The effector $CD8^+$ T cells were cultured in 6-well plates at 0.625 10^6 cells/mL in complete DMEM/F-F12 medium with 1 µg/mL anti-CD28 (clone H37.51). The 6-well plates were coated with 3 µg/mL anti-CD3ε (145-2C11) in PBS 4 h at 37°C and washed three time with PBS before seeding the T cells. Cells were cultured for 48 h (37°C, 7.5% CO_2), after which IL-2 (PeproTech) was added to a final concentration of 10 U/mL. The cells were then cultured for a further 48 h.

Generation and production of PhyB

PhyB is produced in BL21(DE3) *E. coli* (Sigma Aldrich) transfected with three plasmids provided by Dr. K. Rosen [23] that encode the heme oxygenase 1 (Ho1), phytochromobilin (PΦB) synthase lacking the transit peptide (ΔHY2), and Phytochrome B ($PhyB_{1\text{-}651}$). The latter was modified to add a Strep-tag at the C terminus of $PhyB_{1\text{-}651}$. Alternatively, we used the plasmid pMH1105 [24], a gift from Dr Wilfried Weber (Addgene, plasmid # 131864 ; http://n2t.net/addgene:131864 ; RRID:Addgene_131864) to produce a biotinylated form of PhyB; this plasmid encodes the $PhyB_{1\text{-}651}$, HO1 and PCB:ferredoxin oxidoreductase (PcyA). For the production of PhyB, the transfected bacteria were grown at 30°C in

lysogeny broth medium supplemented with the selection antibiotics, then induced with 1 mM Isopropyl-β-D-1-thiogalactopyranoside (IPTG) at OD 600 nm between 0.6 and 0.8 and grown overnight at 18°C in the dark at 150 rpm. For biotinylated PhyB production, biotin was added (5 µM) to the culture medium allowing the biotinylation of the Avi-Tag. Bacteria were harvested by centrifugation 8 min at 6,500 g at 4°C, then resuspended in lysis buffer (50 mM HEPES, 500 mM NaCl, 5% glycerol, 0.5 mM TCEP, 20 mM imidazole, pH 7.4) and shock freeze in liquid nitrogen before to be stored at -80°C. Bacteria were disrupted by adding DNASE (10 µg/mL) and $MgSO_4$ (20 mM) during 20 min and then sonicated. Lysate was cleared from debris by centrifugation at 30,000 g at 4°C for 30 min before to be loaded onto a Ni-NTA Superflow cartridge (Qiagen) using an Äkta Explorer chromatography system (GE Healthcare) and purified. The purified protein buffer was exchanged to PBS containing 0.5 mM TCEP using a HiPrep 26/10 desalting column (GE Healthcare).

Generation and production of the LiTe

The LiTe protein is produced by coexpressing the genes encoding for the H57 Fab Light Chain (LC) cloned in pTT22 eukaryotic expression vector (pTT22-H57Fab-LC plasmid), and the one for the H57 Fab Heavy Chain (HC) linked to the PIF6 domain with a 6xHis tag (Supplementary Fig. 1) into the pYD7, eukaryotic expression vector (pYD7-H57Fab-HC-PIF plasmid). All cloning reactions were performed using In-Fusion HD cloning kit (Clontech) in a standard reaction mixture.

Then LiTe protein is produced by transfecting the HEK293T cell line with pYD7-H57Fab-HC-PIF plasmid and pTT22-H57Fab-LC plasmid (ratio 1:3) using polyethylenimine (PEI, Polysciences). Cells were then maintained in DMEM supplemented with 2% FBS, 0.5% Tryptone TN1 (OrganoTechnie), 1.25 mM valproic acid and geneticin, at 37°C with 5% CO2. Supernatants were harvested 7 days later and the protein purified by Ni-NTA affinity chromatography. The purified protein buffer was exchanged to PBS using Slide-A-Lyzer™ Dialysis Cassette (Thermo Fischer).

Western blot analysis

Purified proteins in reduced 5X Laemmli loading buffer were denatured 5 min at 95°C before been loaded on a 10% SDS–PAGE gel, separated by electrophoresis and transfer on nitrocellulose membrane (LI-COR). Membranes were blocked with 4% bovine serum albumin (BSA) in TBS/T buffer (137 mM NaCl, 20 mM Tris pH 7.6, 0.1% Tween 20). Proteins were detected with reagents coupled to HRP, revealed by chemiluminescence with the Pierce™ ECL Western kit (Thermo Scientific™) and Azure biosystems 300 imaging system.

Flow cytometry analysis

Cells were washed twice with FACS buffer (PBS, 0.5% FBS), then incubated for 45 min at 10°C before been labeled with antibodies in FACS buffer. After 3 washes, cells were resuspended in FACS buffer and analyzed by flow cytometry on a BD FACSCanto™. Data were analyzed with FlowJo software (Treestar Inc., CA).

Spectral analysis of PhyB photoswitching

Spectral analysis of PhyB photoswitching was measured with a NanoDrop™ One (Thermo Scientific™). The absorption spectrum of PhyB was measured after 3 min under light exposure at 680 nm. Then, samples were exposed to 740 nm light for 1 h before recording a new absorption spectrum.

Light-controlled PhyB/LiTe pull-down assay

Streptavidin-coated magnetic beads (MagStrep "type3" XT beads 5% suspension, IBA Lifesciences GmbH) were washed three times in PBS supplemented with 0.5 mM TCEP with a magnetic separator

(IBA Lifesciences GmbH). Then, 20 μg/mL of PhyB were incubated with beads for 1 h at 4°C, 3 times washed before the addition of the LiTe protein at a concentration of 20 μg/mL. The mix samples were illuminated 10 min with a light at 656 nm or 740 nm. After 3 washes, the samples were boiled and the eluted proteins analyzed by western blotting.

Photostimulations and calcium imaging

A 20 μg/mL solution of PhyB protein was added to washed streptavidin-coated polystyrene beads (5.0-5.9 μm, Spherotech Inc.), then incubated 1 h on ice. After washing in PBS supplemented with 0.5 mM TCEP, the beads were resuspended in complete DMEM/F-12 medium without phenol-red and distributed in Lab-Tek™ II chamber coverglass (Thermo Fisher™). Primary T lymphocytes were loaded with PBX calcium reporter according to manufacturer's instructions, washed before been incubated with 20 μg/mL of LiTe protein per conditions during 45 min at room temperature, washed, and incubated with PhyB-coated beads. The samples were illuminated with a 656nm or 740nm LED system (MIGHTEX) and imaged by videomicroscopy, at 37°C.

T cell activation analyses

A 20 μg/mL solution of PhyB protein was added to washed streptavidin-coated polystyrene beads and then incubated for 1 h in ice. After washing with PBS supplemented with 0.5 mM TCEP, the beads were resuspended in complete DMEM/F-12 medium. The beads were distributed in black clear-bottom 96-well plate (Greiner). Plates were illuminated on optoPlate for 3 min under a 780 nm light to ensure a closed conformation of all PhyB proteins. Primary T cells labeled with 0.3 μg/mL of LiTe protein were added at a concentration of 5 10^5 cells/well in presence of 2 μg/mL anti-CD28 antibody. The plates were incubated on the optoPlate located in cell culture incubator, and exposed to the indicated photostimulation programs. The harvested T cells were then analyzed for cell surface protein expression by flow cytometry, and their supernatants for cytokine secretion. IL-2 production has been analyzed by ELISA. Plates were read at 450 nm with Infinite M1000 PRO® (Tecan). IFN-γ, TNF-α and IL-17A were detected by multiplex analysis (Legend-plex, Biolegend) and read with a cytometer Canto II (Becton-Dickinson).

Melanoma targeted PhyB generation and enrichment

Biotinylated PhyB has been added to a streptavidin solution in PBS/TCEP with 2:1 molar ratio under constant vortexing before the addition of an excess of biotinylated TA-99 antibody. Samples were separated by HPLC, and the protein content evaluated by absorbance at 280 nm and 680 nm for total protein and PhyB detection, respectively. The collected fractions were then analyzed by Western blot and revealed with streptavidin-HRP to detect biotinylated proteins.

Measurement of light-induced tumor cell killing by flow cytometry

A total of 2.10^5 melanoma B16F10 cells per well were plated in a 96-well plate and loaded with the Melanoma targeted PhyB. Effector $CD8^+$ T cells were cocultured at 10:1 ratio with the target cells in a total volume of 200 μl/well of RPMI supplemented with 10% FBS, 1 mM NaPy, 10 mM HEPES, 0.05 mM β2-mercapto-ethanol and the LiTe protein (0.3 μg/mL). Cells were illuminated with the indicated light for 18 h at 37°C. Then, the CTL/target cells ratio, identified respectively with an anti-CD45 and an anti-TRP-1 mAb, were determined by flow cytometry.

Statistical analyses

Quantitative data were reported as means ± SD or ± SEM. Excel (Microsoft) and Prism (GraphPad Software) were used for statistical analyses. The non-parametric Wilcoxon-Mann-Whitney test or the Student t test were used for the evaluation of significance, as indicated in the figures. The sample number (*N*) refers to the number of biological replicates. n.s. = not significant ($P > 0.05$), *$P < 0.05$, **$P < 0.01$, ***$P < 0.001$ and ****$P < 0.0001$.

ACKNOWLEDGMENTS

We thank J.M. Ingargiola from the Institut des Sciences du Mouvement and Dr. S. Mailfert from the PICSL imaging facility of the CIML (ImagImm), for the construction of the optoPlate, Drs Leung and Rosen for plasmids encoding PhyB and related enzymes, Drs Horner and Weber for advices and plasmid for PhyB production, A. Formisano for AF488-H57-597 Fab generation and coupling, Dr L. Gauthier for TA-99 antibody supply and for advices, C. Debarnot for advices in protein production. We thank the CIML cytometry platforms for technical and methodological support. We acknowledge the PICSL imaging facility of the CIML (ImagImm), member of the national infrastructure France-BioImaging supported by the French National Research Agency (ANR-10-INBS-04). **Funding**: This work was supported by institutional funding from the French National Institute of Health and Medical Research (Inserm), Centre National de la Recherche Scientifique (CNRS), and Aix-Marseille-Université (AMU), and program grants from the French National Research Agency (ANR-14-CE14-0014-01 to R.L.; ANR-18-CE15-0021-02 to D.M., ANR-17-CE15-0032 to H.T.H) and SATT Sud-Est (SATT N°191702 to D.M.). M. J. was funded by fellowship from INSERM/ Région SUD/Innate Pharma (RSE18003AAA), and by the French Foundation for Medical Research (FRM: FDT202106013223). **Author contribution:** M.J, A.A, S.B, R.L designed the study, performed the experiments and analyzed the results. F.D, R.V, R.C, R.J.A, M.B, M.L assisted in the realization and interpretation of the experiments. R.L supervised and direct the research. R.L, H-T.H, D.M participate in the acquisition of the financial supports of the project. R.L, D.M, M.J wrote the manuscript. All authors discussed the results and contributed to editing of the manuscript. **Competing interests:** The authors declare no competing interests. Patent application PCT/EP2019/076914 and EP22305545.0 corresponding respectively to the LiTe and the LiTe-Me systems have been filed. **Data and materials availability:** All data needed to evaluate the conclusions in the paper are present in the paper and/or Supplementary Materials. Additional data related to this paper may be requested from the authors.

REFERENCES

1. Purvis, J.E. & Lahav, G. Encoding and decoding cellular information through signaling dynamics. *Cell* **152**, 945-956 (2013).
2. Hugues, S. et al. Distinct T cell dynamics in lymph nodes during the induction of tolerance and immunity. *Nat Immunol* **5**, 1235-1242 (2004).
3. Mempel, T.R., Henrickson, S.E. & Von Andrian, U.H. T-cell priming by dendritic cells in lymph nodes occurs in three distinct phases. *Nature* **427**, 154-159 (2004).
4. Moreau, H.D. & Bousso, P. Visualizing how T cells collect activation signals in vivo. *Curr Opin Immunol* **26**, 56-62 (2014).
5. Friedman, R.S., Beemiller, P., Sorensen, C.M., Jacobelli, J. & Krummel, M.F. Real-time analysis of T cell receptors in naive cells in vitro and in vivo reveals flexibility in synapse and signaling dynamics. *J Exp Med* **207**, 2733-2749 (2010).
6. Faroudi, M., Zaru, R., Paulet, P., Muller, S. & Valitutti, S. Cutting edge: T lymphocyte activation by repeated immunological synapse formation and intermittent signaling. *J Immunol* **171**, 1128-1132 (2003).
7. Clark, C.E., Hasan, M. & Bousso, P. A role for the immediate early gene product c-fos in imprinting T cells with short-term memory for signal summation. *PLoS One* **6**, e18916 (2011).

8. O'Donoghue, G.P. et al. T cells selectively filter oscillatory signals on the minutes timescale. *Proc Natl Acad Sci U S A* **118** (2021).
9. Harris, M.J., Fuyal, M. & James, J.R. Quantifying persistence in the T-cell signaling network using an optically controllable antigen receptor. *Mol Syst Biol* **17**, e10091 (2021).
10. Marangoni, F. et al. The transcription factor NFAT exhibits signal memory during serial T cell interactions with antigen-presenting cells. *Immunity* **38**, 237-249 (2013).
11. Yousefi, O.S. et al. Optogenetic control shows that kinetic proofreading regulates the activity of the T cell receptor. *Elife* **8** (2019).
12. Tischer, D.K. & Weiner, O.D. Light-based tuning of ligand half-life supports kinetic proofreading model of T cell signaling. *Elife* **8** (2019).
13. Bohineust, A., Garcia, Z., Corre, B., Lemaitre, F. & Bousso, P. Optogenetic manipulation of calcium signals in single T cells in vivo. *Nature communications* **11**, 1143 (2020).
14. Zhao, B. et al. An Optogenetic Controllable T Cell System for Hepatocellular Carcinoma Immunotherapy. *Theranostics* **9**, 1837-1850 (2019).
15. Huang, Z. et al. Engineering light-controllable CAR T cells for cancer immunotherapy. *Sci Adv* **6**, eaay9209 (2020).
16. Joshi, J., Rubart, M. & Zhu, W. Optogenetics: Background, Methodological Advances and Potential Applications for Cardiovascular Research and Medicine. *Front Bioeng Biotechnol* **7**, 466 (2019).
17. Mijares, A., Lebesgue, D., Wallukat, G. & Hoebeke, J. From agonist to antagonist: Fab fragments of an agonist-like monoclonal anti-beta(2)-adrenoceptor antibody behave as antagonists. *Mol Pharmacol* **58**, 373-379 (2000).
18. Huse, M. et al. Spatial and temporal dynamics of T cell receptor signaling with a photoactivatable agonist. *Immunity* **27**, 76-88 (2007).
19. Varma, R., Campi, G., Yokosuka, T., Saito, T. & Dustin, M.L. T cell receptor-proximal signals are sustained in peripheral microclusters and terminated in the central supramolecular activation cluster. *Immunity* **25**, 117-127 (2006).
20. Bugaj, L.J. & Lim, W.A. High-throughput multicolor optogenetics in microwell plates. *Nature protocols* **14**, 2205-2228 (2019).
21. Bansal, A., Shikha, S. & Zhang, Y. Towards translational optogenetics. *Nat Biomed Eng* (2022).
22. Sadoun, A. et al. Controlling T cells spreading, mechanics and activation by micropatterning. *Scientific reports* **11**, 6783 (2021).
23. Leung, D.W., Otomo, C., Chory, J. & Rosen, M.K. Genetically encoded photoswitching of actin assembly through the Cdc42-WASP-Arp2/3 complex pathway. *Proc Natl Acad Sci U S A* **105**, 12797-12802 (2008).
24. Horner, M., Yousefi, O.S., Schamel, W.W.A. & Weber, W. Production, Purification and Characterization of Recombinant Biotinylated Phytochrome B for Extracellular Optogenetics. *Bio Protoc* **10**, e3541 (2020).